

THE UNIVERSITY OF MICHIGAN
COLLEGE OF ENGINEERING

Department of Meteorology and Oceanography

Technical Report

ON THE INFLUENCE OF THE LOWER BOUNDARY
CONDITION ON BAROCLINIC STABILITY

A. Wiin-Nielsen

ORA Project 00263

supported by:

NATIONAL SCIENCE FOUNDATION
GRANT NO. GA-16166
WASHINGTON, D.C.

administered through

OFFICE OF RESEARCH ADMINISTRATION

ANN ARBOR

December 1970

TABLE OF CONTENTS

	Page
LIST OF FIGURES	iv
ABSTRACT	vi
1. INTRODUCTION	1
2. BOUNDARY CONDITIONS	3
3. THE QUASI-GEOSTROPHIC CASE	5
3.1 The Case $dU/dp_* = \text{const.} < 0, \sigma = \beta = 0$	7
3.2 The Case $dU/dp_* = \text{const.} < 0, \beta = \text{const.}, \sigma = 0$	15
3.3 The Case $dU/dp_* = \text{const.} < 0, \beta = 0, \sigma = \text{const.} > 0$	22
4. THE GENERAL CASE	30
5. THE TWO-LEVEL MODEL	33
6. CONCLUSIONS	40
REFERENCES	43

LIST OF FIGURES

Figure	Page
1. Phase speed as a function of wavelength for the case $\sigma = \beta = U_0 = 0$ and $dU/dz = 2 \text{ m sec}^{-1} \text{ km}^{-1}$.	10
2. Curves of equal e-folding time in a diagram with wavelength as abscissa and windshear as ordinate for the case $\sigma = \beta = U_0 = 0$.	11
3. Neutral curves for the case $\sigma = \beta = 0$ for the improved boundary condition. Stability below the curves and instability above them.	12
4. Phase speed as a function of wavelength for the case $\sigma = \beta = 0$ and $dU/dz = 2 \text{ m sec}^{-1} \text{ km}^{-1}$.	13
5. Curves of equal e-folding time in a diagram with wavelength as abscissa and windshear as ordinate for the case $\sigma = \beta = 0$ and $U_0 = 5 \text{ m sec}^{-1}$	13
6. Percentage change in the e-folding time as a function of wavelength caused by changing the boundary condition for the case $\sigma = \beta = U_0$ and $dU/dz = 2 \text{ m sec}^{-1} \text{ km}^{-1}$.	15
7. Curves of equal e-folding time for the case $\sigma = 0, \beta \neq 0$, and $U_0 = 10 \text{ m sec}^{-1}$.	19
8. Percentage change of e-folding as a function of wavelength caused by changing the lower boundary condition for the case $\sigma = 0, \beta \neq 0, U_0 = 10 \text{ m sec}^{-1}$ and $dU/dz = 2 \text{ m sec}^{-1} \text{ km}^{-1}$.	19
9. The phase speed as a function of wavelength for the case $\sigma = 0, \beta \neq 0, U_0 = 10 \text{ m sec}^{-1}$ and $dU/dz = 2 \text{ m sec}^{-1} \text{ km}^{-1}$.	21
10. Curves of equal e-folding time for the case $\sigma \neq 0, \beta = 0, U_0 = 10 \text{ m sec}^{-1}$ using the improved boundary condition.	25

LIST OF FIGURES (Concluded)

Figure	Page
11. Curves of equal e-folding time for the case $\sigma \neq 0$, $\beta = 0$, $U_0 = 10 \text{ m sec}^{-1}$ using the simplified lower boundary condition.	26
12. Percentage change in e-folding time as a function of wavelength caused by changing the lower boundary condition for the case $\sigma \neq 0$, $\beta = 0$, $U_0 = 10 \text{ m sec}^{-1}$, $dU/dz = 2 \text{ m sec}^{-1} \text{ km}^{-1}$.	27
13. Percentage change in e-folding time as a function of wavelength caused by changing the lower boundary condition for the case $\sigma \neq 0$, $\beta = 0$, $U_0 = 0$, $dU/dz = 2 \text{ m sec}^{-1} \text{ km}^{-1}$.	28
14. The phase speed as a function of wavelength for the case $\sigma \neq 0$, $\beta = 0$, $U_0 = 10 \text{ m sec}^{-1}$, $dU/dz = 2 \text{ m sec}^{-1} \text{ km}^{-1}$.	
15. The phase speed as a function of wavelength for the case $\sigma \neq 0$, $\beta = 0$, $U_0 = 0$, $dU/dz = 2 \text{ m sec}^{-1} \text{ km}^{-1}$.	
16. Percentage change in the e-folding time of the unstable waves caused by changing the lower boundary condition for the two-level, quasi-geostrophic model.	38
17. Phase speed as a function of wavelength for the two-level, quasi-geostrophic model for the case $U_* = 20 \text{ m sec}^{-1}$ and $dU/dz = 2 \text{ m sec}^{-1} \text{ km}^{-1}$.	39

ABSTRACT

The quasi-geostrophic, baroclinic instability problem has been solved using two different boundary conditions at the earth's surface, approximated by a constant pressure surface. A simplified boundary condition, $\omega = 0$ at $p = p_0$, has been used in earlier investigations. The more realistic boundary condition of $w = 0$ at $p = p_0$ is used in this study. Comparisons are made between the speed of propagation of the waves and the instability of the zonal flow for the two boundary conditions.

Four different simple cases are considered. In all cases a linear profile with respect to pressure of the basic zonal wind is used. The first case excludes the effects of the variation of the earth's rotation (the beta effect) and the effects of the static stability parameter. These effects are added to the model, one by one, in the second and the third cases. The last case includes both of these effects in a two-level, quasi-geostrophic model.

The first case shows a reduction of the phase speed and an increase of the instability for all wavelengths, when we use the more realistic boundary condition. When the beta effect is included, we find an increase in the instability at relatively short waves, while the effect of the static stability turns out to be an increase of the instability in an intermediate band of wavelengths. Due to the fact that there is only a small region in common for the two bands where an increase in instability is found, we find that

the improved boundary condition results in stabilization almost everywhere in the model where both effects are included.

The major effect of the improved lower boundary condition is the significant reduction of the retrogression of the very long waves.

1. INTRODUCTION

The purpose of this paper is to describe the results of some studies of baroclinic instability. The baroclinic instability problem has been treated by numerous authors. A comprehensive bibliography of such studies is given by Derome and Wiin-Nielsen (1966). Common to all the studies is the assumption that the vertically averaged flow is nondivergent. This assumption is usually incorporated in the study in one of two different ways. If height is used as the vertical coordinate it is customary to consider a model of finite height bounded below by a flat rigid plate simulating the surface of the earth and above by another rigid plate simulating the presence of a very stable stratosphere. The vertical velocity, $w = dz/dt$, is zero at both of the two boundary surfaces, and if the flow is assumed to be incompressible, it follows that the vertical mean flow is nondivergent. On the other hand, if pressure is used as the vertical coordinate it is customary to use the boundary conditions $\omega = dp/dt = 0$ for $p = 0$ (the outer boundary of the atmosphere) and $p = p_0$, where p_0 is a standard surface pressure for the atmosphere. Under these conditions it follows from the continuity equation that the vertical mean flow, averaged with respect to pressure, is nondivergent.

In this study we shall use pressure as the vertical coordinate. The boundary condition $\omega = 0$ for $p = p_0$ is introduced in theoretical studies for mathematical convenience. It is, however, conceivable that some modifications of the results of baroclinic instability studies will appear if

the boundary condition at the lower boundary is replaced by a more realistic condition. It is the purpose of this study to investigate the importance of the lower boundary condition for the stability characteristics of the large-scale atmospheric flow. It is known that a change in the lower boundary condition will create significant changes in the speed of propagation of atmospheric waves, especially if the waves have a large wavelength (Eliassen and Machenhauer, 1969; Wiin-Nielsen, 1970a, 1970b). The main effect is created by the nonvanishing, vertical mean divergence in the model. While the vertical mean divergence is crucial for the explanation of the speed of propagation of very long transient atmospheric waves, it may only have minor effects on the stability characteristics of the flow because the very long waves are either stable or weakly unstable due to the stabilizing influence of the rotation of the earth.

2. BOUNDARY CONDITIONS

The boundary condition at the outer boundary of the atmosphere will be $\omega = 0$ for $p = 0$. The condition at the lower boundary is $w = 0$ if we consider a flat earth. We make the approximation that the condition $w = 0$ can be applied to a constant pressure surface close to the ground (Phillips, 1963). The condition can therefore be written in the form

$$g\omega = \frac{d\phi}{dt} = \frac{\partial\phi}{\partial t} + \vec{v} \cdot \nabla\phi + \omega \frac{\partial\phi}{\partial p} = 0, \quad p = p_0 \quad (2.1)$$

where g is the acceleration of gravity, $\phi = gz$ the geopotential, \vec{v} the horizontal wind and $\omega = dp/dt$. (2.1) takes a particularly simple form if the flow is considered to be quasi-geostrophic. Under this condition we get:

$$\omega = \rho \frac{\partial\phi}{\partial t}, \quad p = p_0 \quad (2.2)$$

where we have made use of the hydrostatic assumption, and where ρ is the density. If we assume that the perturbations are of the form $\exp(ik(x - ct))$ we get from (2.2)

$$\hat{\omega} = -ikc \frac{p_0}{RT_0} \hat{\phi}, \quad p = p_0 \quad (2.3)$$

where $\hat{\omega}$ and $\hat{\phi}$ are the amplitudes of the vertical velocity and the geopotential, respectively, R the gas constant and T_0 the temperature at $p = p_0$.

If the model is more general than the quasi-geostrophic model, we get a more complicated condition from (2.1). Assuming that the basic state is characterized by a zonal flow $U = U(p)$ and a geopotential $\phi = \phi(y, p)$, and that the basic flow is geostrophic, i. e.,

$$fU = - \frac{\partial \phi}{\partial y} \quad (2.4)$$

we get from (2.1)

$$\frac{\partial \phi}{\partial t} + U \frac{\partial \phi}{\partial x} - fUv + \omega \frac{\partial \phi}{\partial p} = 0, \quad p = p_0 \quad (2.5)$$

where the lower case letters denote perturbation quantities. Assuming again that the basic state is in hydrostatic equilibrium, and that the perturbations are of the same form we get:

$$\hat{\omega} = \frac{p_0}{RT_0} [ik (U - c) \hat{\phi} - fU\hat{v}], \quad p = p_0 \quad (2.6)$$

The conditions (2.3) and (2.6) can in some cases be expressed entirely in terms of the vertical velocity and its first derivative at $p = p_0$ depending upon the form of the perturbations and the particular model under investigation. We shall return to this question later in connection with the various cases which will be treated in the following sections.

3. THE QUASI-GEOSTROPHIC CASE

In this section we shall consider the same quasi-geostrophic model as was treated by Derome and Wiin-Nielsen (1966). The basic nonlinear equations for the model are:

$$\frac{\partial \zeta}{\partial t} + \vec{v} \cdot \nabla (\zeta + f) = f_o \frac{\partial \omega}{\partial p} \quad (3.1)$$

$$\frac{\partial}{\partial t} \left(\frac{\partial \psi}{\partial p} \right) + \vec{v} \cdot \nabla \left(\frac{\partial \psi}{\partial p} \right) + \frac{\sigma}{f_o} \omega = 0 \quad (3.2)$$

where the notations are the same as in the earlier paper. Assuming as before a basic state characterized by a zonal wind $U = U(p)$ and perturbations of the form

$$\psi(x, p, t) = \hat{\psi}(p) e^{ik(x - ct)} \quad (3.3)$$

$$\omega(x, p, t) = \hat{\omega}(p) e^{ik(x - ct)} \quad (3.4)$$

where we note that both the zonal current and the perturbations have been assumed to be independent of y , the meridional coordinate, we get from (3.1) and (3.2)

$$ik \left[c - U + c_R \right] \hat{\psi} - \frac{f_o}{k^2} \frac{d\hat{\omega}}{dp} = 0 \quad (3.5)$$

$$-ik(c - U) \frac{d\hat{\psi}}{dp} - ik \frac{dU}{dp} \hat{\psi} + \frac{\sigma}{f_o} \hat{\omega} = 0 \quad (3.6)$$

where $c_R = \beta/k^2$.

When $\hat{\psi}$ is eliminated from (3.5) and (3.6), and when we introduce the nondimensional independent variable $p_* = p/p_0$ we get the following equation for $\hat{\omega}$:

$$(c - U)(c - U + c_R) \frac{d^2 \hat{\omega}}{dp_*^2} + [2(c - U) + c_R] \frac{dU}{dp_*} \frac{d\hat{\omega}}{dp_*} - \frac{c_g^2}{c_I^2} (c - U + c_R)^2 \hat{\omega} = 0 \quad (3.7)$$

where $c_g^2 = \sigma p_0^2$ and $c_I = f_0/k$.

The boundary conditions for (3.7) are $\hat{\omega} = 0$, $p_* = 0$ and (2.3) at $p_* = 1$.

It is now possible to express (2.3) entirely in $\hat{\omega}$. In formulating the basic Eqs. (3.1) and (3.2) it was assumed that $\phi = f_0 \psi$. From (2.3) we get therefore

$$\hat{\omega} + ikc \frac{p_0}{RT_0} f_0 \hat{\psi} = 0, p_* = 1 \quad (3.8)$$

We may now substitute from (3.5) into (3.8) and thereby eliminate $\hat{\psi}$ from the boundary condition. We get

$$\hat{\omega} + \frac{p_0}{RT_0} \frac{c_I^2 c}{c - U + c_R} \frac{d\hat{\omega}}{dp} = 0 \quad (3.9)$$

or

$$\frac{d\hat{\omega}}{dp_*} + \frac{RT_o}{c_I^2} \frac{c - U + c_R}{c} \hat{\omega} = 0, p_* = 1 \quad (3.10)$$

(3.10) is the boundary condition replacing the condition $\hat{\omega} = 0, p_* = 1$ in the quasi-geostrophic case. In the following we shall consider various cases which already have been solved using the simplified boundary condition in order to see how the more realistic boundary condition effects the speed of propagation of the waves and the stability of the zonal current. The following cases were treated by Derome and Wiin-Nielsen (1966):

- (a) $dU/dp = 0, \beta = \text{const.}, \sigma = \text{const.}$
- (b) $dU/dp = \text{const.} < 0, \beta = 0, \sigma = 0.$
- (c) $dU/dp = \text{const.} < 0, \beta = \text{const.}, \sigma = 0.$
- (d) $dU/dp = \text{const.} < 0, \beta = 0, \sigma = \text{const.}$

In this paper we shall consider the cases (b), (c), and (d). Case (a) has been considered in detail by Wiin-Nielsen (1970a) together with other cases characterized by a distribution of $\sigma = \sigma(p)$ corresponding to a constant lapse rate.

3.1 THE CASE $dU/dp_* = \text{const.} < 0, \sigma = \beta = 0$

The solution of (3.7) in this case using the simplified boundary condition $\hat{\omega} = 0, p_* = 1$ gives the result that the waves will move with a speed equal to the zonal current at the level $p_* = 0.5$ and that the zonal current is unstable for all wavelengths. The general solution to (3.7) in this case is

$$\hat{\omega}(p_*) = A(p_* - 1 + c_*)^3 + B \quad (3.11)$$

where it is assumed that the basic current has the form

$$U(p_*) = U_o + U_T (1 - p_*) \quad (3.12)$$

and

$$c_* = \frac{c - U_o}{U_T} \quad (3.13)$$

In order to satisfy the boundary condition at $p_* = 0$ we must have:

$$(c_* - 1)^3 A + B = 0 \quad (3.14)$$

while the boundary condition at $p_* = 1$, i.e., Eq. (3.10), leads to the condition

$$3Ac_*^2 + \frac{RT_o}{c_I^2} \frac{U_T c_*}{U_o + U_T c_*} (Ac_*^3 + B) = 0 \quad (3.15)$$

If (3.14) and (3.15) shall have nontrivial solutions the determinant must vanish. This condition leads to the equation

$$3U_T(1 + q)c_*^2 - 3(U_T - qU_o)c_* + U_T = 0 \quad (3.16)$$

where we have introduced the notation

$$q = \frac{c_I^2}{RT_o}$$

The solution to (3.16) may be written in the form

$$c_* = \frac{U_T - qU_o}{2U_T(1+q)} \pm \frac{\sqrt{D}}{2U_T(1+q)} \quad (3.17)$$

where

$$D = q^2 U_o^2 - 2qU_oU_T - \frac{1}{3}(1+4q)U_T^2 \quad (3.18)$$

We see from (3.17) and (3.18) that if $q = 0$, which corresponds to the simplified boundary condition, we get

$$c_* = \frac{1}{2} \pm i\frac{\sqrt{3}}{6} \quad (3.19)$$

(3.19) is the solution analyzed earlier by Derome and Wiin-Nielsen (1966), and it is seen that one always gets an unstable solution, while the speed of propagation is equal to the speed at the level $p_* = 0.5$. We note furthermore from (3.18) that if $U_o = 0$ we still get unstable solutions for all values of the wavelength and the vertical windshear. In this case the solution is

$$c_* = \frac{1}{2(1+q)} \pm i \frac{\sqrt{3(1+4q)}}{6(1+q)} \quad (3.20)$$

or

$$c = \frac{U_T}{2(1+q)} \pm i \frac{U_T}{6} \frac{\sqrt{3(1+4q)}}{(1+q)} \quad (3.21)$$

A comparison between (3.19) and (3.20) shows that both the speed of propagation and the degree of instability are changed. Figure 1 shows the speed of propagation as a function of wavelength computed from (3.21) for $dU/dz = 2 \text{ m sec}^{-1} \text{ km}^{-1}$. The effect of the more realistic lower boundary condition

is to decrease the wave speed by very significant amounts for long waves.

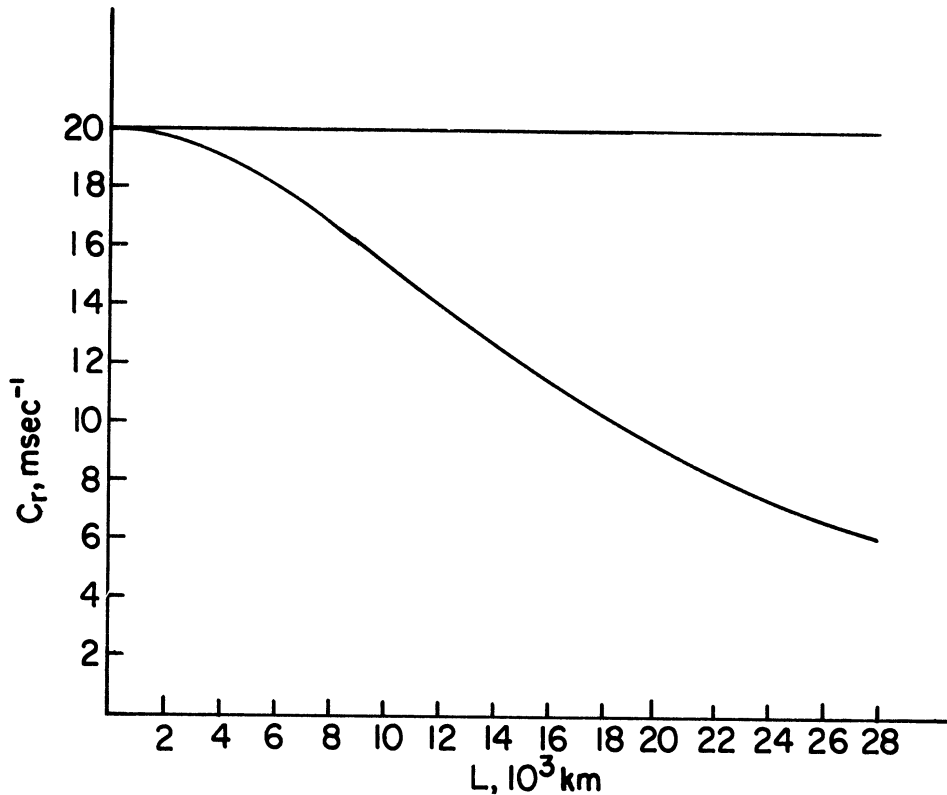


Figure 1. Phase speed as a function of wavelength for the case $\sigma = \beta = U_0 = 0$ and $dU/dz = 2 \text{ m sec}^{-1} \text{ km}^{-1}$.

Figure 2 shows a comparison between the e-folding times computed from (3.19) and (3.20). The results show that the effect of the improved boundary condition is to make the zonal current more unstable for almost all wavelengths. It can be seen that the improved boundary condition will stabilize the very longest waves. From (3.19) and (3.20) it can easily be shown that stabilization will take place for all wave lengths larger than $25.5 \times 10^3 \text{ km}$, or equivalently $q > 2$.

We consider next the case where $U_0 > 0$. It is seen from (3.18) that D is no longer everywhere negative. This means that the effect of a westerly zonal current at the surface ($p_* = 1$) is to stabilize the zonal current.

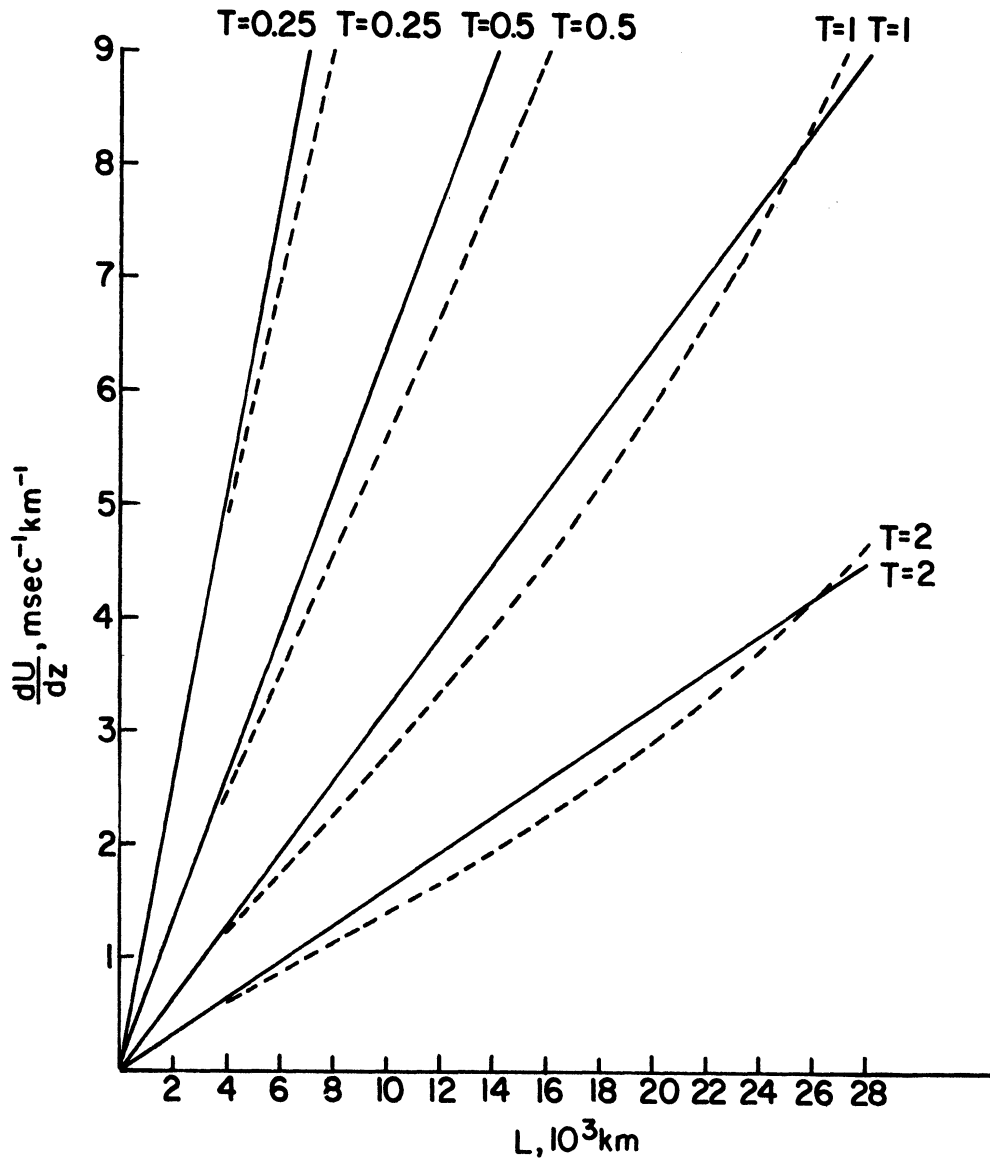


Figure 2. Curves of equal e-folding time in a diagram with wavelength as abscissa and windshear as ordinate for the case $\sigma = \beta = U_0 = 0$. Solid lines correspond to the simplified boundary condition and dashed lines to the improved boundary condition.

This effect is shown in Figure 3 for the values $U_0 = 5 \text{ m sec}^{-1}$ and $U_0 = 10 \text{ m sec}^{-1}$. The region below the curves indicates stability, while instability is present above the curves. It is also seen from Figure 3 that stability occurs only for rather small values of the windshear, and that instability would occur for observed values of the vertical windshear.

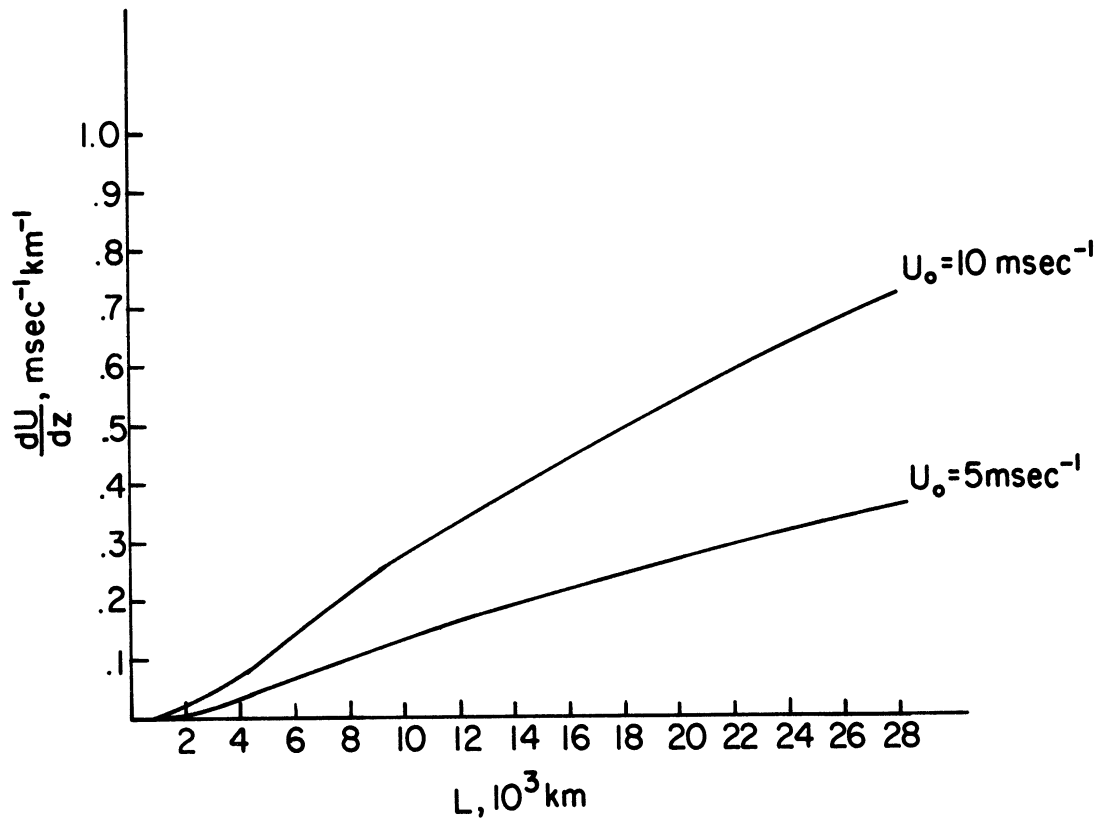


Figure 3. Neutral curves for the case $\sigma = \beta = 0$ for the improved boundary condition. Stability below the curves and instability above them.

The speed of propagation of the waves is influenced by the improved boundary condition in essentially the same way as when $U_0 = 0$. Figure 4 shows c_r as a function of wavelength when $U_0 = 10 \text{ m sec}^{-1}$ and $dU/dz = 2 \text{ m sec}^{-1} \text{ km}^{-1}$. We find again the reduction of the speed of propagation resulting from the lower boundary condition.

We consider next the unstable waves in the case $U_0 > 0$. Figure 5 presents in the customary way isolines for the e-folding time in a diagram with wavelength as abscissa and the vertical windshear as ordinate. The dashed lines are computed from the simplified boundary condition ($\omega = 0$, $p_* = 1$) while the solid lines result from the improved boundary condition

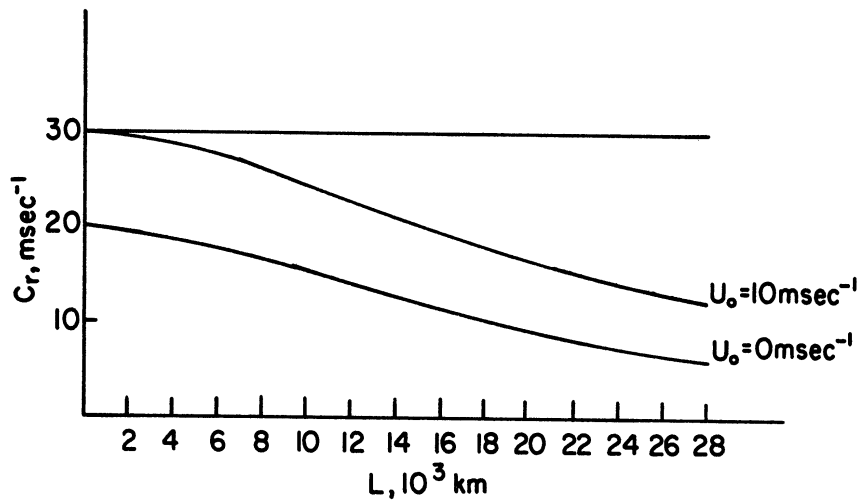


Figure 4. Phase speed as a function of wavelength for the case $\sigma = \beta = 0$ and $dU/dz = 2 \text{ m sec}^{-1} \text{ km}^{-1}$. The horizontal line corresponds to the simplified lower boundary condition.

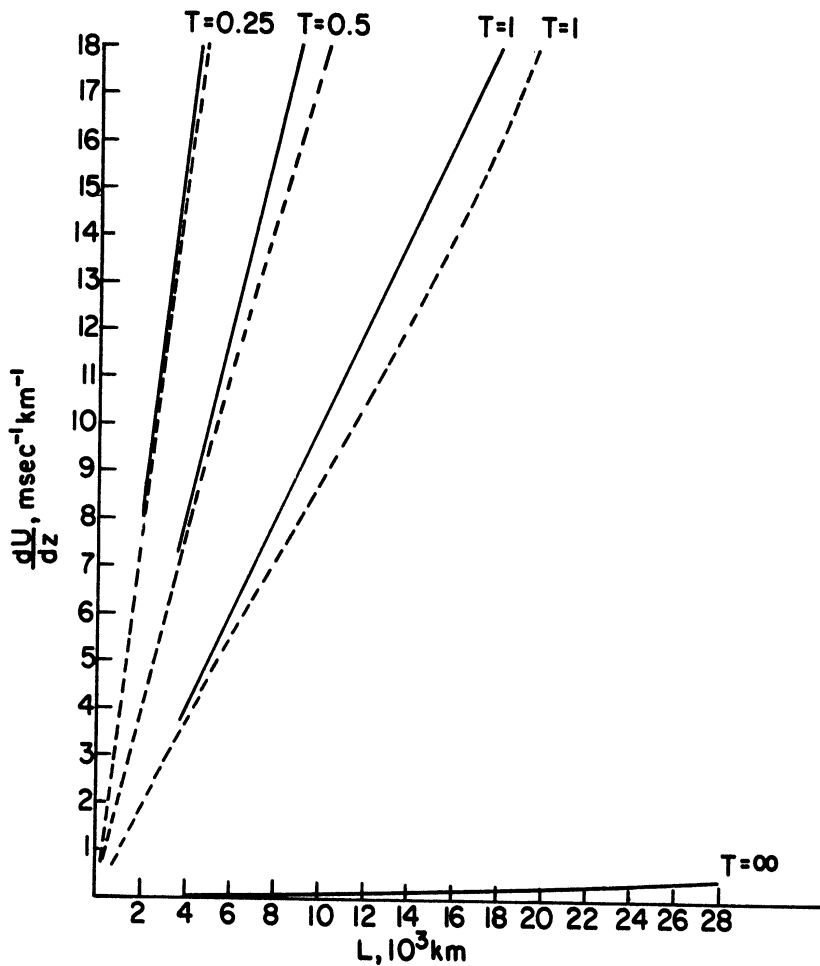


Figure 5. Curves of equal e-folding time in a diagram with wavelength as abscissa and windshear as ordinate for the case $\sigma = \beta = 0$ and $U_0 = 5 \text{ m sec}^{-1}$. Solid lines correspond to the simplified lower boundary condition and dashed lines to the improved condition.

($w = 0$, $p_* = 1$). Figure 5 displays essentially the same result as Figure 2 which corresponded to the case $U_0 = 0$, i.e., that the improved boundary condition in the region of meteorological interest results in a destabilization of the flow as seen from the curves for $T = 0.25, 0.5,$ and 1 day. The curve separating the unstable from the stable region is reproduced from Figure 3. It is obvious that the simple statement made above cannot be true in the region of the neutral curve, because the model using the simplified boundary condition will result in unstable condition, while the improved boundary condition gives stability. In any case, the instability in this region is always extremely weak if present at all.

In order to illustrate the difference in the degree of instability between the two boundary conditions we have prepared Figure 6 which shows the percentage change in the e-folding time between the two boundary conditions for $U_0 = 0$. We note from Figure 6 that the relative change is the largest around $L = 13 \times 10^3$ km and amounts to about 15%. There is a stabilization for very long waves in this case just as we found in Figure 2.

The present case which does not include the beta effect and the effect of static stability is not very realistic from a meteorological point of view. However, it shows probably most clearly the effects of changing the lower boundary condition and has therefore been included in the paper. Based upon this case we can conclude that the effect of the improved lower boundary condition coupled with a nonvanishing zonal wind at the surface will create a region of stability for very small values of the vertical windshear. However, for values of the windshear comparable to those observed in the

atmosphere we find an increase in the instability.

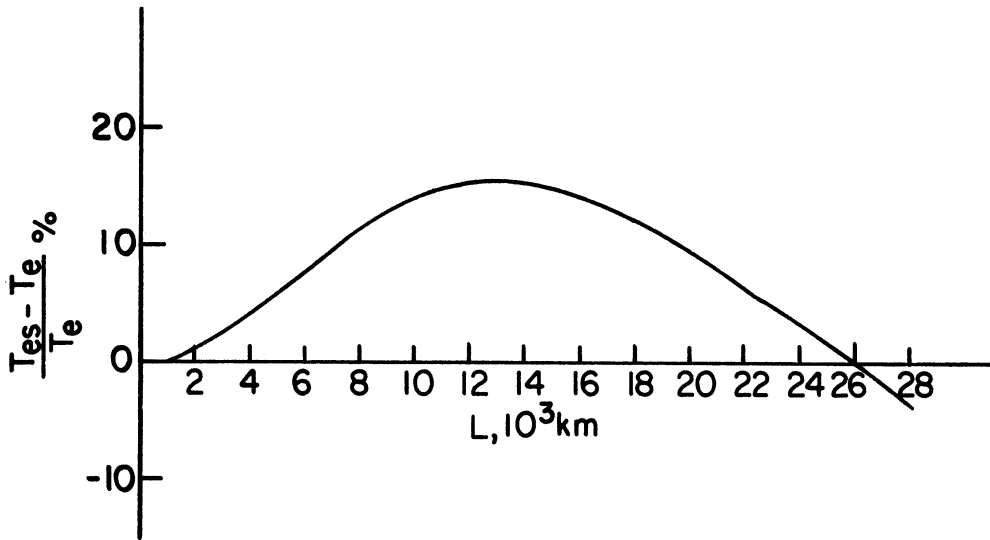


Figure 6. Percentage change in the e-folding time as a function of wavelength caused by changing the boundary condition for the case $\sigma = \beta = U_0 = 0$ and $dU/dz = 2 \text{ m sec}^{-1} \text{ km}^{-1}$.

3.2 THE CASE $dU/dp_* = \text{const.} < 0$, $\beta = \text{const.}$, $\sigma = 0$

The differential equation to be solved in this case is

$$(c - U)(c - U + c_R) \frac{d^2 \hat{\omega}}{dp_*^2} + [2(c - U) + c_R] \frac{dU}{dp_*} \frac{d\hat{\omega}}{dp_*} = 0 \quad (3.22)$$

as seen from (3.7) by putting $c_g^2 = \sigma p_0^2$ equal to zero. The solution to (3.22) can be obtained from the paper by Derome and Wiin-Nielsen (1966), but as shown by Wiin-Nielsen (1967), it is also possible to solve (3.22) under the more general condition of a completely arbitrary zonal wind profile $U = U(p)$ in the basic state. Adopting the latter procedure we find from (3.22) that

$$\frac{d\hat{\omega}}{dp} = A(U - c)(U - c - c_R) \quad (3.23)$$

and therefore

$$\hat{\omega} = A \int_0^{p_*} (U - c)(U - c - c_R) dp_* \quad (3.24)$$

where we already have incorporated the boundary condition $\hat{\omega} = 0$, $p_* = 0$. The phase speed c is now determined from the lower boundary condition (3.10) at $p_* = 1$. Denoting

$$I_1 = \int_0^1 U dp_* \quad (3.25)$$

and

$$I_2 = \int_0^1 U^2 dp_* \quad (3.26)$$

we find from (3.10)

$$\begin{aligned} (U_0 - c)(U_0 - c - c_R) + \frac{1}{q} \frac{c - U_0 + c_R}{c} [I_2 - 2 I_1 c + c^2 \\ - c_R I_1 + c_R c] = 0 \end{aligned} \quad (3.27)$$

where q as before is

$$q = \frac{c_I^2}{RT_0} \quad (3.28)$$

Since (3.27) has a common factor of $(c - U_0 + c_R)$ we find one solution to be

$$c = U_0 - c_R \quad (3.29)$$

while the remaining solution can be determined from the quadratic equation

$$(1 + q)c^2 - (2I_1 - c_R + qU_o)c + (I_2 - c_R I_1) = 0 \quad (3.30)$$

The solution to (3.30) can be written in the form

$$c = \frac{2I_1 - c_R + qU_o}{2(1 + q)} \pm \frac{\sqrt{D}}{2(1 + q)} \quad (3.31)$$

where

$$D = (2I_1 - c_R + qU_o)^2 - 4(1 + q)(I_2 - c_R I_1) \quad (3.32)$$

While the formulas (3.31) and (3.32) can be evaluated for an arbitrary wind profile we shall restrict ourselves to the profile

$$U = U_o + U_T(1 - p_*) \quad (3.33)$$

for the purposes of comparison. We get

$$I_1 = U_o + \frac{1}{2} U_T \quad (3.34)$$

and

$$I_2 = U_o^2 + U_o U_T + \frac{1}{3} U_T^2$$

We get therefore

$$c = \frac{U_T + (2 + q)U_o - c_R}{2(1 + q)} \pm \frac{\sqrt{D}}{2(1 + q)} \quad (3.35)$$

where

$$D = -\frac{1}{3}(1 + 4q)U_T^2 + 2q(c_R - U_o)U_T + [c_R^2 + q^2U_o^2 + 2qc_R U_o] \quad (3.36)$$

The region of instability can be obtained from (3.36) by determining the conditions under which $D < 0$. In that region we may calculate the e-folding time from the definition:

$$kc_i T_e = 1 \quad (3.37)$$

and since

$$c_i = \frac{\sqrt{-D}}{2(1+q)} \quad (3.38)$$

we obtain

$$-D = \frac{4(1+q)^2}{k^2 T_e^2} \quad (3.39)$$

It is seen from (3.36) that D is quadratic in U_T and it is therefore a straightforward matter to calculate the isolines for T_e . Figure 7 is the stability diagram where the isolines are shown in a coordinate system with wavelength as abscissa and the vertical windshear as ordinate. The solid lines correspond to the simplified boundary condition ($\omega = 0, p_* = 1$), while the dashed lines were computed from improved boundary condition with $U_0 = 10 \text{ m sec}^{-1}$ ($\omega = 0, p_* = 1$). It is seen that the improved boundary condition results in an increase in instability everywhere, and that no great change is observed in the stabilizing effect of the beta term. We may again give a measure of the difference in instability by computing the percentage change in e-folding time for a given windshear and surface wind. The result of such a calculation is shown in Figure 8, computed with $U_0 = 0$ and $dU/dz = 2 \text{ m sec}^{-1} \text{ km}^{-1}$. It is seen that the percentage change is relatively small except when the wavelength approaches the neutral curve.

Our next concern is to investigate the speed of propagation of the waves in this model. As a representative example we have selected a case where

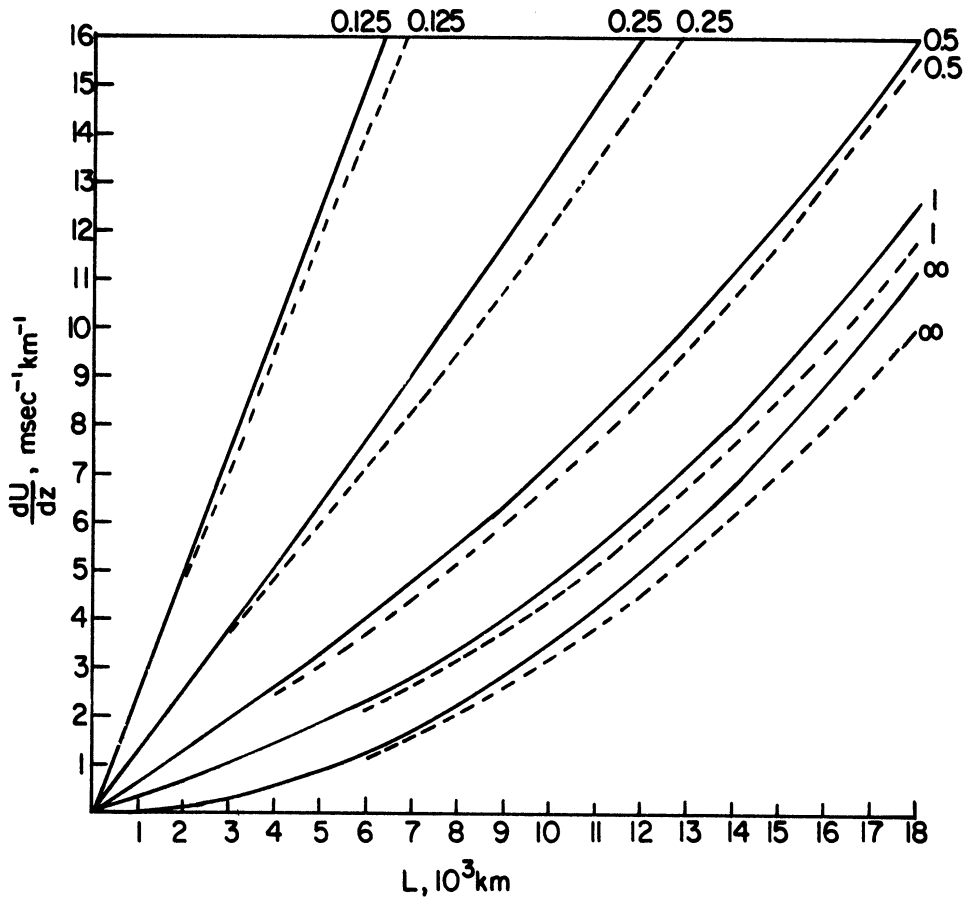


Figure 7. Curves of equal e-folding time for the case $\sigma = 0$, $\beta \neq 0$ and $U_0 = 10 \text{ m sec}^{-1}$. Arrangement as in Figure 2.

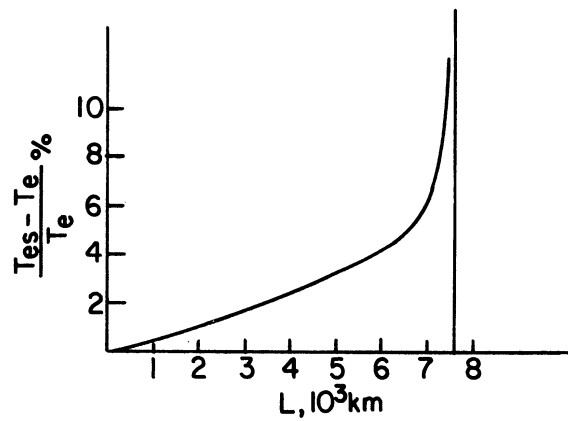


Figure 8. Percentage change of e-folding as a function of wavelength caused by changing the lower boundary condition for the case $\sigma = 0$, $\beta \neq 0$, $U_0 = 0$, $dU/dz = 2 \text{ m sec}^{-1} \text{ km}^{-1}$.

$dU/dz = 2 \text{ m sec}^{-1} \text{ km}^{-1}$ and $U_0 = 10 \text{ m sec}^{-1}$. The result of the calculation is displayed in Figure 9, where we also have included the curves (marked s) obtained when we have $q = 0$. In the unstable region we have only one value of the speed of propagation. It is seen that only minor changes are found in the speed of propagation for this range of wavelengths when the simple boundary condition is replaced by the improved condition. On the other hand, in the stable region we have two values of the speed of propagation. Only minor changes are caused by the change of the boundary condition for the branch which correspond to positive values of c_r , and the two values for this branch will be the same as the wavelength goes to infinity. Major changes are found for the branch which corresponds to negative values of c_r for sufficiently long waves. When $q = 0$ it has been shown earlier that the values of c_r on the negative branch behave in the same way as nondivergent, barotropic Rossby waves, i.e., according to the formula

$$c = U - c_r \quad (3.40)$$

However, when $q \neq 0$, it is seen that the negative values of c_r are greatly reduced in magnitude caused by the improved boundary condition. This effect has been studied in greater detail by Wiin-Nielsen (1970, 1970b), and it was shown that the improved boundary condition results in a much more realistic behavior of the waves for large values of the wavelength.

In conclusion we may state that the major effect of the improved lower boundary condition is to reduce the retrogression of the very long waves.

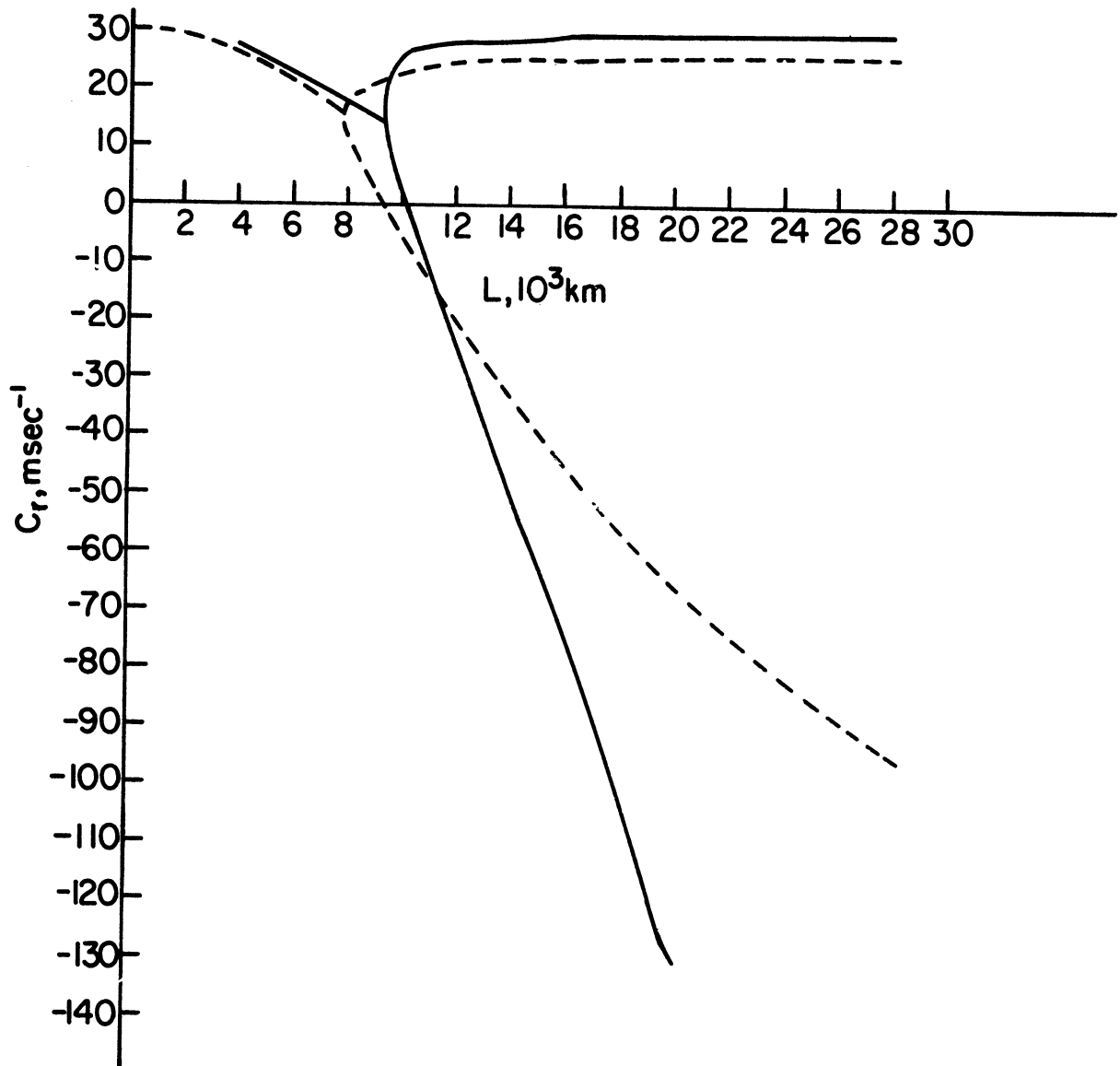


Figure 9. The phase speed as a function of wavelength for the case $\sigma = 0$, $\beta \neq 0$, $U_0 = 10 \text{ m sec}^{-1}$ and $dU/dz = 2 \text{ m sec}^{-1} \text{ km}^{-1}$. Solid lines correspond to the simplified boundary condition and dashed lines to the improved condition.

The stability of the flow is affected in such a way that most waves, except the very long waves, become slightly more unstable, but the change in e-folding time for a given value of the windshear is in no case very large. It should finally be pointed out that the examples displayed in Figures 7, 8, and 9 were computed for specific values of U_0 . Other values

values of $U_0 < 10 \text{ m sec}^{-1}$ were also investigated, and the results are identical to those displayed here for all practical purposes indicating that the stability is almost independent of the strength of the zonal current at the surface ($p_* = 1$). The most important quantity is the vertical windshear.

3.3 THE CASE $dU/dp_* = \text{const.} < 0$, $\beta = 0$, $\sigma = \text{const.} > 0$

The differential equation to be solved in this case is obtained from (3.7) by setting $c_R = 0$. We obtain

$$(c - U) \frac{d^2 \hat{\omega}}{dp_*^2} + 2 \frac{dU}{dp_*} \frac{d \hat{\omega}}{dp_*} - \frac{c^2 g}{c_I^2} (c - U) \hat{\omega} = 0 \quad (3.41)$$

Using again the wind profile

$$U = U_0 + U_T(1 - p_*) \quad (3.42)$$

and defining

$$c_* = \frac{c - U_0}{U_T} \quad (3.43)$$

it was shown by Derome and Wiin-Nielsen (1966) that the solution to (3.41)

is

$$\hat{\omega} = A(s\xi \sinh(s\xi) - \cosh(s\xi)) + B(s\xi \cosh(s\xi) - \sinh(s\xi)) \quad (3.44)$$

where

$$s^2 = \frac{c^2 g}{c_I^2} \quad (3.45)$$

$$\text{and } \xi = p_* - 1 + c_* \quad (3.46)$$

The boundary conditions are

$$\hat{\omega} = 0, p_* = 0, \xi = c_* - 1 \quad (3.47)$$

and

$$\frac{d\hat{\omega}}{d\xi} + \frac{c - U_o}{c} \frac{1}{q} \hat{\omega} = 0, p_* = 1, \xi = c_* \quad (3.48)$$

or

$$\frac{d\hat{\omega}}{d\xi} + \frac{U_T c_*}{U_T c_* + U_o} \frac{1}{q} \hat{\omega} = 0, p_* = 1, \xi = c_* \quad (3.49)$$

When the solution (3.44) is substituted into the boundary conditions (3.47) and (3.49) we obtain two linear homogeneous equations in A and B. If these equations shall have nontrivial solutions, the determinant must vanish. After considerable manipulation we obtained a quadratic equation for the determination of c_* . This equation can be written in the form:

$$D_2 c_*^2 + D_1 c_* + D_0 = 0 \quad (3.50)$$

where

$$\begin{aligned} D_2 &= sU_T \left(1 + \frac{1}{sq} \tanh s\right) \\ D_1 &= s(U_o - U_T) + U_T \left(1 - \frac{1}{q}\right) \tanh s \\ D_0 &= \left(U_o - \frac{U_T}{2}\right) (\tanh s - s) \end{aligned} \quad (3.51)$$

(3.50) has been solved in a large number of cases varying the wavelength and the vertical windshear in a systematic way. Having obtained c_* through

this procedure the e-folding time was computed from the formula:

$$T_e = \frac{1}{kc_i} \quad (3.52)$$

The result is presented in Figure 10 which shows isolines for the e-folding time in a diagram with wavelength as abscissa and vertical wind-shear as ordinate. Figure 10 was constructed using $U_0 = 10 \text{ m sec}^{-1}$. Figure 11 shows an analogous diagram computed with the simple boundary condition $\omega = 0, p_* = 1$. A comparison between Figure 10 and Figure 11 shows that the improved boundary condition creates a region of stability for all wavelengths and sufficiently small vertical windshears. We note in addition that there are significant changes in the instability for very long waves. The improved boundary condition results in larger e-folding times, i.e., a smaller degree of instability for the very long waves. It can also be detected from the two figures that the reverse situation occurs for the short waves where the improved boundary condition results in a larger degree of instability. These differences in the instability are more clearly demonstrated by plotting the percentage change in the e-folding time as a function of wavelength for a constant value of the vertical windshear. Figure 12 shows this quantity computed for the value $U_0 = 10 \text{ m sec}^{-1}$. It is seen that the degree of instability is increased by about 20% for intermediate wavelengths, but decreased by as much as 80% for the longest wavelengths included in this study. Similar curves are obtained for other values of U_0 , but the percentage change in the e-folding time is somewhat smaller for the smaller values of U_0 .

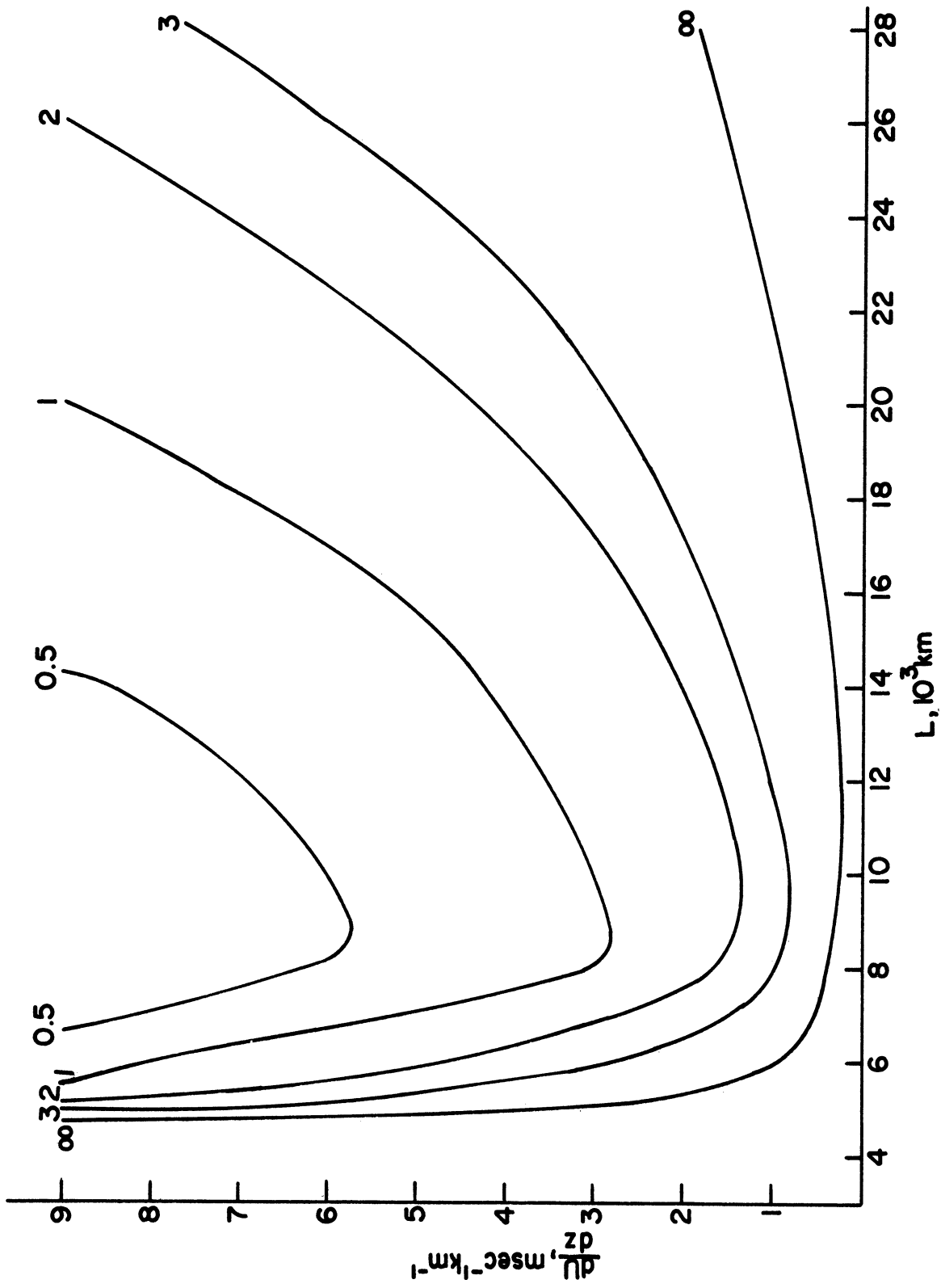


Figure 10. Curves of equal e-folding time for the case $\sigma \neq 0$, $\beta = 0$, $U_0 = 10 \text{ m sec}^{-1}$ using the improved boundary condition. Arrangement as in Figure 2.

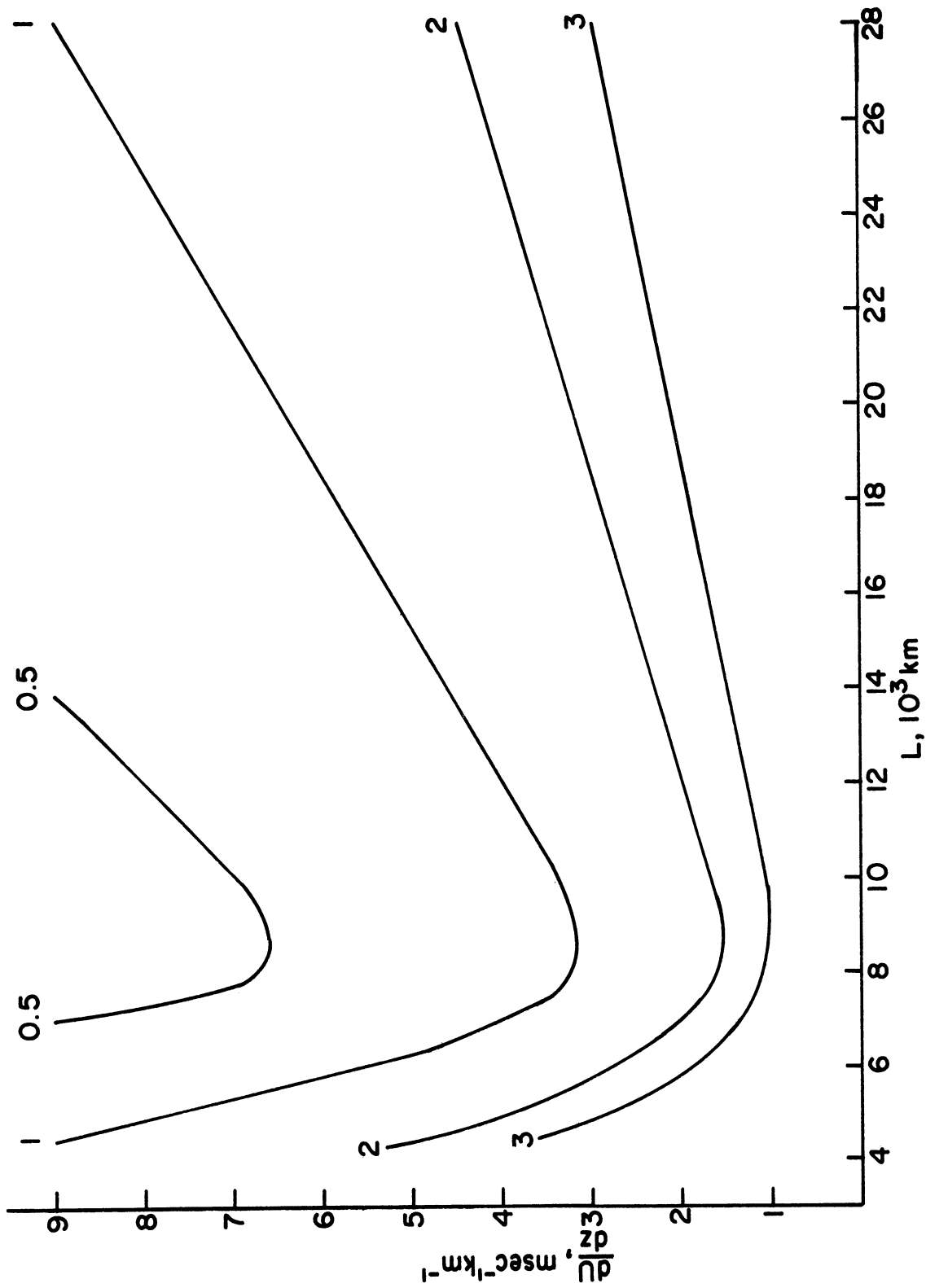


Figure 11. Curves of equal e-folding time for the case $\sigma \neq 0$, $\beta = 0$, $U_0 = 10 \text{ m sec}^{-1}$ using the simplified lower boundary condition.

This effect is seen in Figure 13 which corresponds to the case $U_0 = 0$.

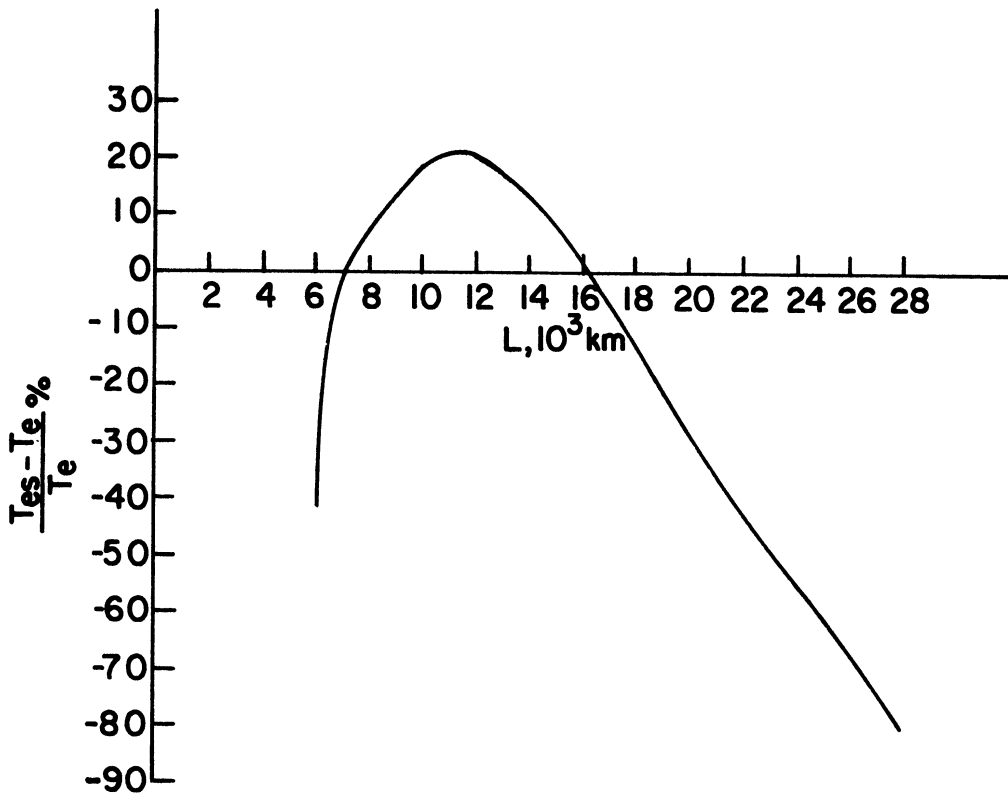


Figure 12. Percentage change in e-folding time as a function of wavelength caused by changing the lower boundary condition for the case $\sigma \neq 0$, $\beta = 0$, $U_0 = 10 \text{ m sec}^{-1}$, $dU/dz = 2 \text{ m sec}^{-1} \text{ km}^{-1}$.

We shall next consider the speed of propagation as influenced by the lower boundary condition. From the solution obtained for the simplified boundary condition at $p_* = 1$ by Derome and Winn-Nielsen (1966) it was noticed that the speed of propagation of the unstable waves is equal to the value of the zonal current at $p_* = 0.5$. As can be expected from the results given in section 3.1 of this paper (see Figure 1 and Figure 4) we will find a change in this aspect of the solution. Figure 14 shows the speed of propagation for the case where $U_0 = 10 \text{ m sec}^{-1}$ and $dU/dz = 2 \text{ m sec}^{-1} \text{ km}^{-1}$. The dashed line on the figure shows the phase speed for the case of the simplified

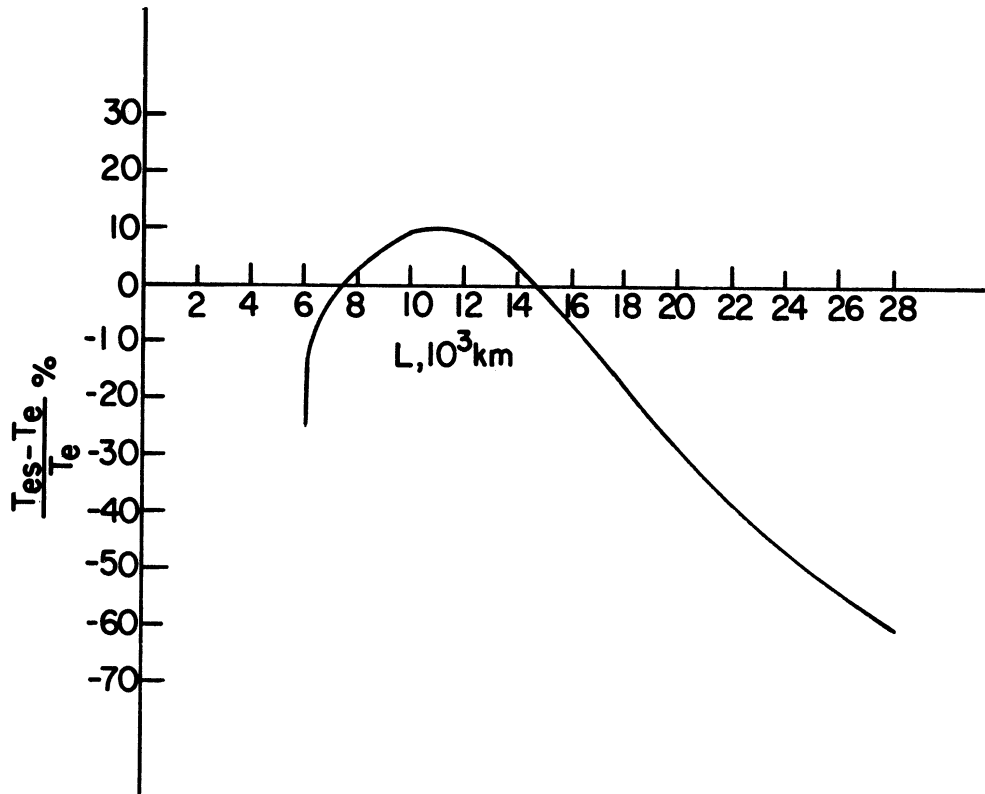


Figure 13. Percentage change in e-folding time as a function of wavelength, caused by changing the lower boundary condition for the case $\sigma \neq 0$, $\beta = 0$, $U_0 = 0$, $dU/dz = 2 \text{ m sec}^{-1} \text{ km}^{-1}$.

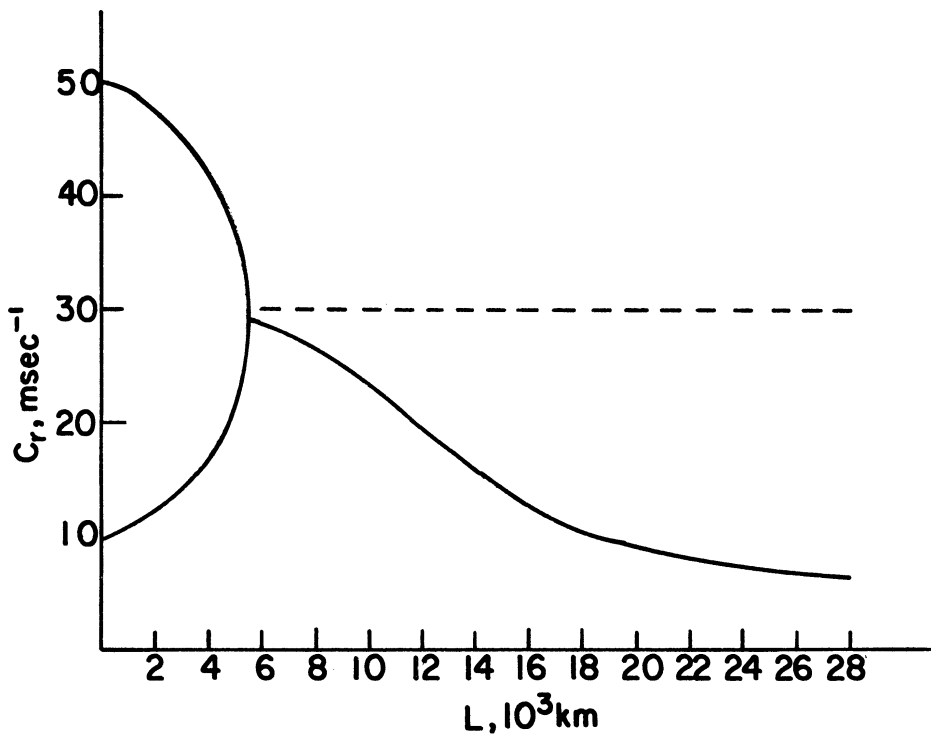


Figure 14. The phase speed as a function of wavelength for the case $\sigma \neq 0$, $\beta = 0$, $U_0 = 10 \text{ m sec}^{-1}$, $dU/dz = 2 \text{ m sec}^{-1} \text{ km}^{-1}$. The dashed line gives the phase speed of the unstable waves if the simplified boundary condition is used.

lower boundary condition and for the region of instability. In the region of stability there are only very minor changes in the phase speed. Analogous changes to those displayed in Figure 14 are found for other values of the parameters U_0 and dU/dz . Figure 15 shows the phase speed when $U_0 = 0$ and the parameters are otherwise as in Figure 14. It is seen that the effect of reducing the phase speed for long waves is created by the more realistic lower boundary condition, but does not depend in an important way on the surface wind speed.

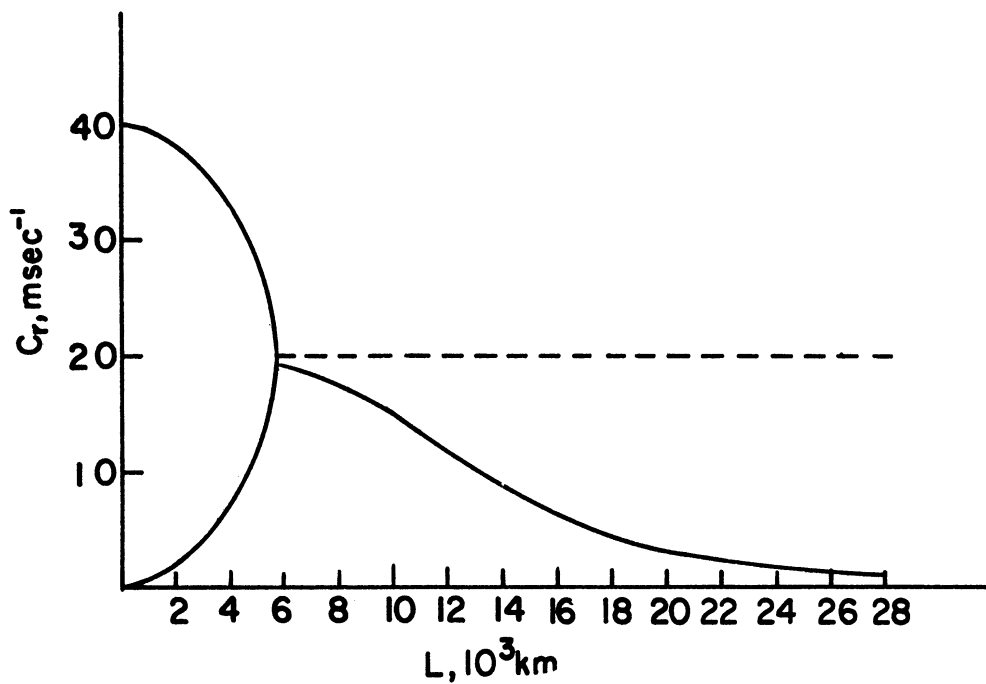


Figure 15. The phase speed as a function of wavelength for the case $\sigma \neq 0$, $\beta = 0$, $U_0 = 0$, $dU/dz = 2 \text{ m sec}^{-1} \text{ km}^{-1}$. The dashed line gives the phase speed of the unstable waves if the simplified boundary condition is used.

4. THE GENERAL CASE

The cases treated in the previous section are special cases each of them excluding at least one important parameter. It is naturally desirable to analyze a quasi-geostrophic model which includes all parameters. The general quasi-geostrophic model having a constant vertical windshear and a constant static stability parameter has recently been analyzed in great detail by Garcia and Norscini (1970). They used height as the vertical coordinate, and their model atmosphere was bounded above and below by horizontal rigid plates at which the vertical velocity vanishes. The fundamental differential equation which must be solved in this case is of the confluent hypergeometric type. It can be shown that the case treated by Garcia and Norscini (1970) is analogous to the differential Eq. (3.7) under the assumptions that $U = U(p)$ is a linear function of pressure, as for example given in (3.12), and that σ is equal to a constant. In order to see this analogy we introduce the transformation

$$\xi = 2 \frac{c}{c_I} \frac{g}{U_T} (U - c) \quad (4.1)$$

into (3.7). We notice that

$$\frac{d}{dp_*} = -2 \frac{c}{c_I} \frac{g}{U_T} \frac{d}{d\xi} \quad (4.2)$$

and

$$\frac{d^2}{dp_*^2} = 4 \frac{c^2}{c_I^2} \frac{g^2}{U_T^2} \frac{d^2}{d\xi^2} \quad (4.3)$$

Denoting

$$\alpha = \frac{c_R c_g}{c_I U_T} \quad (4.4)$$

we get from (3.6) that $\hat{\omega}$ must satisfy the equation

$$\xi(\xi - 2\alpha) \frac{d^2 \hat{\omega}}{d\xi^2} - 2(\xi - \alpha) \frac{d\hat{\omega}}{d\xi} - \frac{1}{4} (\xi - 2\alpha)^2 \hat{\omega} = 0 \quad (4.5)$$

Equation (4.5) is the same as the equation solved by Garcia and Norscini (1970), and when we furthermore note that they solve the equation with the boundary condition that the vertical velocity vanishes at both rigid plates, we have a complete analogy if we were to solve (4.5) with the boundary conditions $\hat{\omega} = 0$ at the top and the bottom of the atmosphere. The boundary conditions become

$$\hat{\omega} = 0, p_* = 0, \xi = \xi_0 = 2 \frac{c_g}{c_I U_T} (U_0 + U_T - c) \quad (4.6)$$

and

$$\hat{\omega} = 0, p_* = 1, \xi = \xi_1 = 2 \frac{c_g}{c_I U_T} (U_0 - c) \quad (4.7)$$

which also may be written in the form

$$\hat{\omega} = 0, p_* = 0, \xi_0 = 2 \frac{c_g}{c_I U_T} \left[\frac{1}{2} U_T - (c - (U_0 + \frac{1}{2} U_T)) \right] \quad (4.8)$$

$$\hat{\omega} = 0, p_* = 1, \xi_1 = -2 \frac{c_g}{c_I U_T} \left[\frac{1}{2} U_T + (c - (U_0 + \frac{1}{2} U_T)) \right] \quad (4.9)$$

which is completely equivalent to the boundary conditions used by Garcia and

Norscini (1970) when we notice that they measure the phase speed relative to the mid-level in their model. We may therefore adopt the results for the model treated by Garcia and Norscini (1970) when we use

$$2U_o = U_T \quad (4.10)$$

and the Richardson number

$$\mu^2 = \frac{c^2}{U_T^2} = \frac{\bar{\sigma}_p^2}{U_T^2} \quad (4.11)$$

In this paper we are mainly interested in the influence of the lower boundary condition. If we adopt the condition $\omega = 0$, $p_* = 1$ we may, as pointed out above, use the solution computed by Garcia and Norscini (1970) and applying (4.10) and (4.11) to convert their results to our model. However, if we adopt the boundary condition (3.10) which is more realistic we can no longer use the analogy between the two solutions because of the difference in boundary conditions.

In order to analyze the influence of the lower boundary condition on the speed of propagation and the stability in the general baroclinic case we must either repeat the calculation by Garcia and Norscini (1970) using the boundary condition (3.10) or use another (numerical) method to obtain the desired solutions for the (complex) phase speed. An investigation of this problem will be described in the near future. However, for the moment we shall be satisfied with a consideration of the two-level model.

5. THE TWO-LEVEL MODEL

The purpose of this section is to describe an investigation of the two-level, quasi-geostrophic model using the boundary conditions (3.8) and $\omega = 0$, $p_* = 1$, separately. Before we enter the details of the calculations it may be useful to discuss the results which we may expect based on the previous sections of this paper. The influence of the improved boundary condition is most clearly seen in the figures which display the percentage change in the e-folding time as a function of wavelength for a given value of the vertical windshear. Figure 6 shows that the effect of the improved boundary condition is to destabilize the zonal current for almost all wavelengths when $\sigma = \beta = 0$. However, when we go to the model where $\beta \neq 0$, and $\sigma = 0$ in which case we find a stabilization for disturbances with a sufficiently large wavelength, we find destabilization for short waves only as seen in Figure 8. The model with $\sigma \neq 0$ and $\beta = 0$ predicts, on the other hand, stability for short waves with both boundary conditions. As seen from Figure 12 and Figure 13 we find only destabilization in a relatively small region ($7000 < Km < L < 16000$ Km) for this model. Due to the fact that we have only a very small region in which we would expect destabilization if we superimposed the wavelength intervals in Figure 8 and Figure 13 for the two models, we would expect that a model which has the stabilizing effects of $\sigma \neq 0$ and $\beta \neq 0$ will show a stabilizing effect of the improved boundary condition for most wavelengths. In the following we shall see if

these anticipations are true.

The vorticity equations for the two-level, quasi-nondivergent model are:

$$\frac{\partial \xi_1}{\partial t} + \vec{v}_1 \cdot \nabla(\xi_1 + f) = \frac{f_o}{P} \omega_2 \quad (5.1)$$

$$\frac{\partial \xi_3}{\partial t} + \vec{v}_3 \cdot \nabla(\xi_3 + f) = -\frac{f_o}{P} \omega_2 + \frac{f_o}{P} \omega_4 \quad (5.2)$$

where subscripts 1, 2, 3, and 4 refer to the levels 25, 50, 75, and 100 cb, respectively. Addition and subtraction of (5.1) and (5.2) lead, after division by 2, to the equations

$$\frac{\partial \xi_*}{\partial t} + \vec{v}_* \cdot \nabla(\xi_* + f) + \vec{v}_T \cdot \nabla \xi_T = \frac{f_o}{2P} \omega_4 \quad (5.3)$$

$$\frac{\partial \xi_T}{\partial t} + \vec{v}_* \cdot \nabla \xi_T + \vec{v}_T \cdot \nabla(\xi_* + f) = \frac{f_o}{P} \omega_2 - \frac{f_o}{2P} \omega_4 \quad (5.4)$$

where the subscript $*$ is defined as

$$(\)_* = \frac{1}{2} [(\)_1 + (\)_3] \quad (5.5)$$

while the subscript T is given by

$$(\)_T = \frac{1}{2} [(\)_1 - (\)_3] \quad (5.6)$$

The adiabatic, thermodynamic equation may be written in the form

$$\frac{\partial \psi_T}{\partial t} + \vec{v}_* \cdot \nabla \psi_T - \frac{\sigma_2 P}{2f_0} \omega_2 = 0 \quad (5.7)$$

When ω_2 is eliminated between (5.7) and (5.4) and the equations are linearized assuming a basic state characterized by the constant speeds U_* and U_T we obtain assuming perturbations which depend on x and t only:

$$\frac{\partial \xi_*}{\partial t} + U_* \frac{\partial \xi_*}{\partial x} + \beta \frac{\partial \psi_*}{\partial x} + U_T \frac{\partial \xi_T}{\partial x} = \frac{f_0}{2P} \omega_4 \quad (5.8)$$

$$\frac{\partial}{\partial t} [\xi_T - \lambda^2 \psi_T] + U_* \frac{\partial}{\partial x} [\xi_T - \lambda^2 \psi_T] + U_T \frac{\partial}{\partial x} [\xi_* + \lambda^2 \psi_*] = \frac{f_0}{2P} \omega_4 \quad (5.9)$$

where λ^2 is defined by the relation

$$\lambda^2 = \frac{2f_0^2}{\sigma P^2} \quad (5.10)$$

Using the boundary condition (2.2) we find that

$$\omega_4 = f_0 \rho_0 \frac{\partial \psi_4}{\partial t} \quad (5.11)$$

where we have used the relation $\psi = \phi/f_0$ as before in this study. (5.11) is introduced in (5.8) and (5.9). When we furthermore assume that

$$\psi_4 = \psi_* - 2\psi_T \quad (5.12)$$

and that the perturbations are of the form

$$\psi_* = \hat{\psi}_* e^{ik(x - ct)}, \quad \psi_T = \hat{\psi}_T e^{ik(x - ct)} \quad (5.13)$$

we obtain the equations

$$\left[\left(1 + \frac{s^2}{k^2} \right) c - U_* + c_R \right] \hat{\psi}_* - \left[U_T + 2 \frac{s^2}{k} \right] \hat{\psi}_T = 0 \quad (5.14)$$

$$\begin{aligned} - \left[\left(1 - \frac{\lambda^2}{k^2} \right) U_T + \frac{s^2}{k^2} c \right] \hat{\psi}_* + \left[\left(1 + \frac{\lambda^2 + 2s^2}{k^2} \right) c - \left(1 + \frac{\lambda^2}{k^2} \right) U_* \right. \\ \left. + c_R \right] \hat{\psi}_T = 0 \end{aligned} \quad (5.15)$$

where

$$s^2 = \frac{f_o^2}{RT_o} \quad (5.16)$$

The phase speed c is obtained by solving the equation resulting from the condition that the determinant of the system (5.14) and (5.15) must vanish if nontrivial solutions shall exist. We obtain a quadratic equation in c which easily can be solved. The equation is

$$A_2 c^2 + A_1 c + A_0 = 0 \quad (5.17)$$

where

$$A_2 = \left(1 + \frac{s^2}{k^2} \right) \left(1 + \frac{\lambda^2 + 2s^2}{k^2} \right) - 2 \frac{s^4}{k^4} \quad (5.18)$$

$$\begin{aligned} A_1 = - \left(\left(1 + \frac{s^2}{k^2} \right) \left[\left(1 + \frac{\lambda^2}{k^2} \right) U_* - c_R \right] + \left(1 + \frac{\lambda^2}{k^2} + 2 \frac{s^2}{k^2} \right) (U_* - c_R) \right. \\ \left. + \frac{s^2}{k^2} U_T + 2 \frac{s^2}{k^2} \left(1 - \frac{\lambda^2}{k^2} \right) U_T \right) \end{aligned} \quad (5.19)$$

$$A_0 = \left[\left(1 + \frac{\lambda^2}{k^2} \right) U_* - c_R \right] [U_* - c_R] - \left(1 - \frac{\lambda^2}{k^2} \right) U_T^2 \quad (5.20)$$

The solution to (5.17) is calculated in a grid with the wavelength as abscissa and the vertical windshear as ordinate. Calculations were carried out for the case stated above and for the case, where $s = 0$ everywhere in (5.18) - (5.20). The latter case is the case of the simplified lower boundary condition $\omega = 0$, $p_* = 1$. If (5.17) has a complex root, the e-folding time was also computed.

Figure 16 shows the percentage change in the e-folding time, defined as

$$\frac{T_{es} - T_e}{T_e} \quad (5.21)$$

where T_e is the e-folding time for (5.17) while T_{es} is the corresponding value when $s = 0$ (simplified lower boundary condition, $\omega = 0$, $p_* = 1$). The thick solid line is the neutral line, separating the unstable and the stable region for the case $s = 0$, while the other curves give the value of (5.21). We observe that the more realistic lower boundary condition causes a stabilization for most wavelengths and windshears. The only exception is in the lower right-hand side of the diagram, where destabilization is found in a relatively small region. For the windshears of meteorological interest we find changes of less than 10%, but significantly larger values are found for large windshears and large wavelengths.

Figure 17 shows the wave speed as a function of wavelength for the two

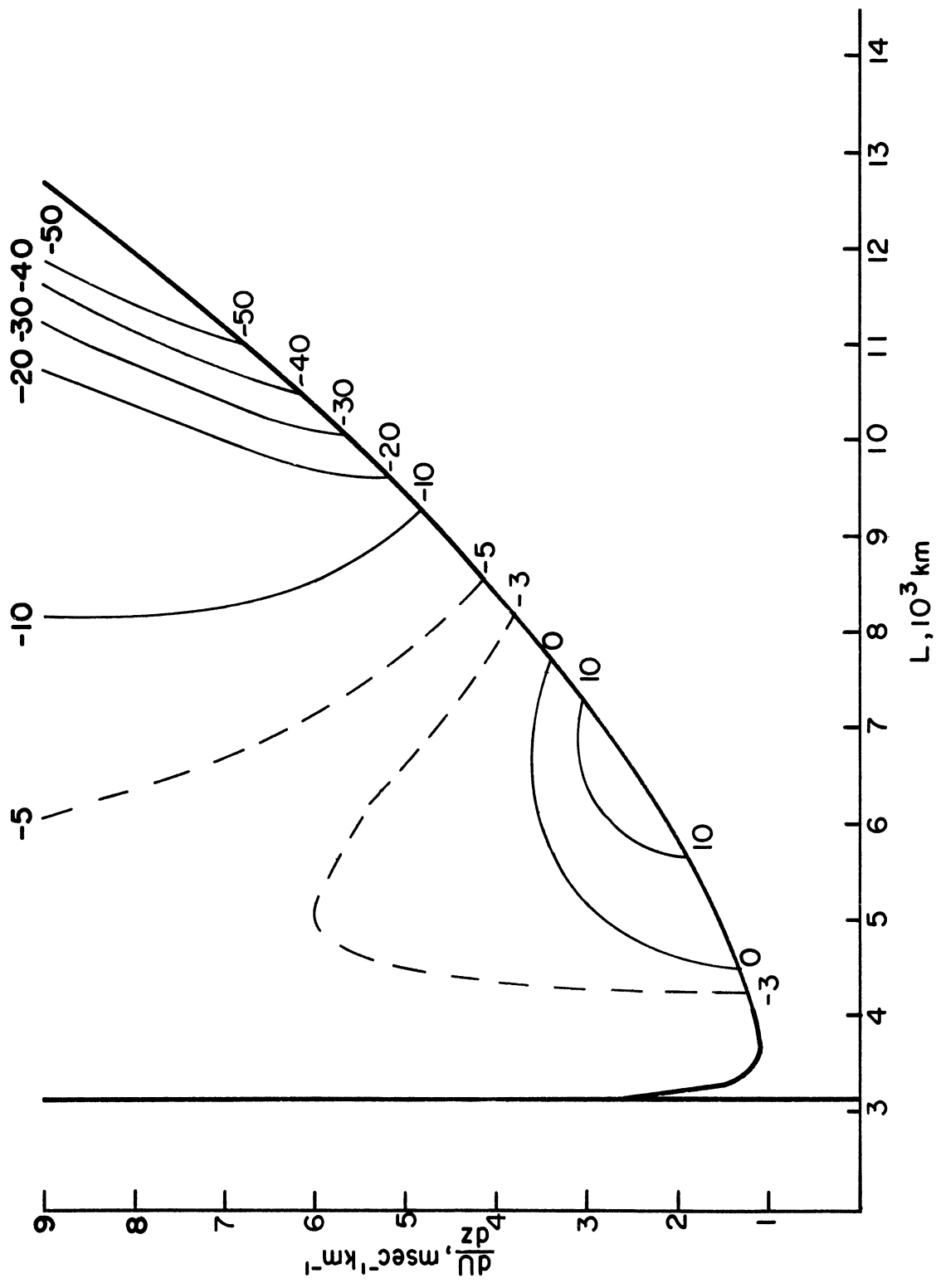


Figure 16. Percentage change in the e-folding time of the unstable waves caused by changing the lower boundary condition for the two-level, quasi-geostrophic model.

lower boundary conditions. This figure indicates that the only important influence of the more realistic lower boundary condition is to decrease the retrogression of the very long waves. A more detailed investigation of this effect has been given by Wiin-Nielsen (1970a, 1970b).

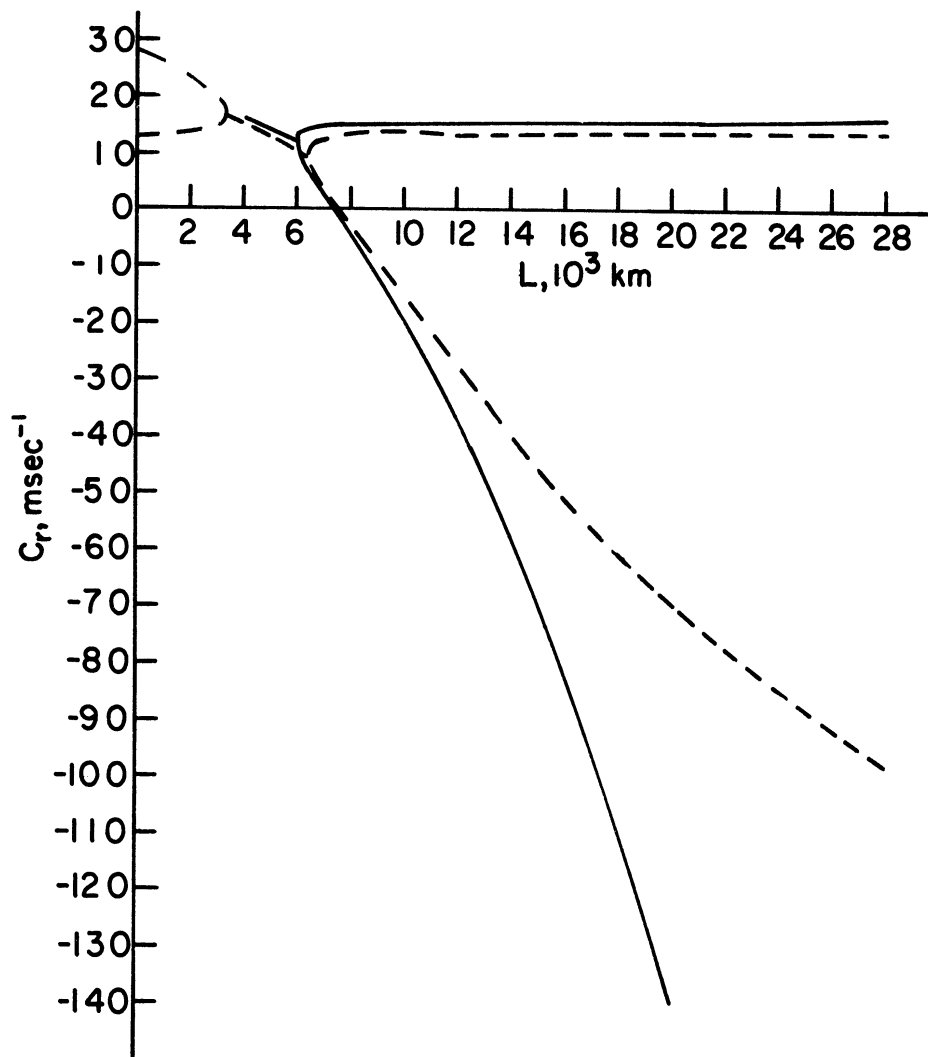


Figure 17. Phase speed as a function of wavelength for the two-level, quasi-geostrophic model for the case $U_* = 20 \text{ m sec}^{-1}$ and $dU/dz = 2 \text{ m sec}^{-1} \text{ km}^{-1}$. Solid lines correspond to the simplified lower boundary condition and dashed lines to the improved boundary condition.

6. CONCLUSIONS

The purpose of this investigation has been to study the effects of changing the lower boundary condition from $\omega = 0$ at $p = p_0$ to $w = 0$ at the same level. In the investigation we have restricted the attention to the quasi-geostrophic model. Several special cases have been studied in order to see the effects of the improved boundary condition.

The simplest case is one in which the beta effect is neglected and where it is assumed that the lapse rate is adiabatic ($\beta = 0, \sigma = 0$). In that case we find that the improved boundary condition results in a destabilization at almost all wavelengths, when the surface wind is zero ($U_0 = 0$). When $U_0 \neq 0$ the effect of the improved boundary condition is to stabilize all wavelengths for sufficiently small values of the vertical windshear.

In the case where $\beta \neq 0$ and $\sigma = 0$ we find for both boundary conditions a stabilization for the long waves. However, in the short wave unstable region the result of changing the lower boundary condition is to destabilize the waves. The improved boundary condition has also the effect to greatly reduce the retrogression of the long stable waves.

The third case, in which $\beta = 0$ and $\sigma \neq 0$, gives the result that all waves longer than a critical wavelength are unstable. However, we find a considerable increase of the e-folding time for very long waves as a result of the improved boundary condition, while a reduction in the e-folding time is found in an intermediate band of the unstable waves.

The general case, in which $\beta \neq 0$ and $\sigma \neq 0$, has not been solved in the model with a continuous variation of the basic zonal current and the static stability parameter, because this case requires considerable amounts of calculations. A later report will consider this case in detail. However, the two-level, quasi-geostrophic model was used to make a preliminary investigation of the general case. As expected from the previous case we find for both boundary conditions a stability diagram similar to the well-known diagram for the two-level model displaying a short wave cut-off due to the effect of the static stability and a long wave cut-off due to the stabilizing beta-effect. However, within the region of instability we find changes in the degree of instability as measured by the e-folding time. For the greater part of the unstable region we find a stabilization which is relatively large for large values of the windshear and the wavelength, but small in the region of maximum instability. A destabilization is found for moderate values of the windshear. The major effect of the improved boundary condition on the wave speed is a considerable reduction of the retrogression of the very long waves.

It should be stressed that the last case should be considered as a preliminary investigation. As shown in section 4 of this paper there is a complete analogy between the general case of $\beta = \text{const.} \neq 0$ and $\sigma = \text{const.} \neq 0$ considered here and the case considered by Garcia and Norscini (1970), when one adopts the simplified boundary condition $\omega = 0$, $p = p_0$. They show that unstable solutions exist for all values of the vertical windshear and the

wavelength although the degree of instability is very small for small values of the wavelength and all values of the windshear and for small values of windshear and all values of the wavelength. Since we have arrived at the result that one of the effects of the improved boundary condition is to act in the direction of stabilization of the very long waves, it is conceivable that the improved boundary condition will change the stability characteristics for the very long waves. In order to answer this question we must solve the general eigenvalue problem using both boundary conditions. The result of such an investigation will be reported later provided a suitable numerical technique for the solution of the problem can be found.

REFERENCES

- Derome, J. F. and A. Wiin-Nielsen: "On the Baroclinic Stability of Zonal Flow in Simple Model Atmospheres," Technical Report, 06372-2-T, The University of Michigan, 93 p. (1966).
- Eliassen, E. and B. Machenhauer: "On the Observed Large-Scale Atmospheric Wave Motion," Tellus, 21, 149-166 (1969).
- Phillips, M. A.: "Geostrophic Motion," Reviews of Geophysics, 1, pp. 123-176 (1963).
- Wiin-Nielsen, A.: "On Baroclinic Instability as a Function of the Vertical Profile of the Zonal Wind," Monthly Weather Review, 95, 733-739, (1967).
- Wiin-Nielsen, A.: "On the Motion of Various Vertical Modes of Transient, Very Long Waves, Part I" (accepted for publication in Tellus) (1970a).
- Wiin-Nielsen, A.: "On the Motion of Various Vertical Modes of Transient, Very Long Waves, Part II" (submitted for publication in Tellus) (1970b).



UNIVERSITY OF MICHIGAN



3 9015 03530 0345